THE AMERICAN SOCIETY OF MECHANICAL ENGINEERS
345 E. 47 St., New York, N.Y. 10017

89-GT-62

Experimental Investigation of Rotor-Stator Interaction in a Centrifugal Pump with Several Vaned Diffusers

N. ARNDT, Research Fellow*
A. J. ACOSTA, Professor
C. E. BRENNEN, Professor
T. K. CAUGHEY, Professor

California Institute of Technology
Pasadena, CA 91125 USA

ABSTRACT

This paper describes an experimental investigation of rotor–stator interaction in a centrifugal pump with several vaned diffusers. Steady and unsteady diffuser vane pressure measurements were made for a two–dimensional test impeller. Unsteady impeller blade pressure measurements were made for a second two–dimensional impeller with blade number and blade geometry identical to the two–dimensional impeller used for the diffuser vane pressure measurements. The experiments were conducted for different flow coefficients and different radial gaps between the impeller blade trailing edge and the diffuser vane leading edge (5% and 8% of the impeller discharge radius). The largest pressure fluctuations on the diffuser vanes and the impeller blades were found to be of the same order of magnitude as the total pressure rise across the pump. The largest pressure fluctuations on the diffuser vanes were observed to occur on the suction side of the vane near the vane leading edge, whereas on the impeller blades the largest fluctuations were observed to occur at the blade trailing edge. However, the dependence of the fluctuations on the flow coefficient was found to be different for the diffuser vanes and the impeller blades; on the vane suction side, the fluctuations were largest for the maximum flow coefficient and decreased with decreasing flow coefficient, whereas at the blade trailing edge, the fluctuations were smallest for the maximum flow coefficient and increased with decreasing flow coefficient. Increasing the number of the diffuser vanes resulted in a significant decrease of the impeller blade pressure fluctuations. The resulting lift on the diffuser vanes was computed from the vane pressure measurements; the magnitude of the fluctuating lift was found to be larger than the steady lift.

INTRODUCTION

Blade and vane design in diffuser pumps, and also in centrifugal compressors, is currently based upon the assumption that the flow in both the impeller and the diffuser is steady. This, however, implies that the radial gap between the impeller discharge and the diffuser inlet is large so that no flow unsteadiness of any kind due to rotor–stator interaction may occur. If, however, the radial gap between the impeller blades and the diffuser vanes is small, i.e., of the order of a small percentage of the impeller discharge radius, as it actually is for many diffuser pumps, there may be a strong interaction that may influence both the aerodynamic and the structural performance of the impeller blades and the diffuser vanes. Cavitation damage observed at the trailing edges of the impeller blades of high–speed centrifugal pumps, such as the High Pressure Oxygen Turbopump (HPOTP) of the Space Shuttle Main Engine (SSME) may also result from fluctuating blade pressures which are due to rotor–stator interaction.

The rotor–stator interaction may be divided into two different mechanisms, potential flow interaction and wake interaction (Dring, 1982). The potential flow interaction between the two blade rows moving relative to each other arises because of the circulation about the blades and because of the potential fields, other than circulation, about the blades that are due to the finite thickness of the blades (Lefcort, 1965). The potential flow fields about a blade extend both upstream and downstream of a blade. The wake interaction refers to the unsteadiness induced at a blade row by the wakes shed by the blades of an upstream blade row and convected downstream. Both potential flow interaction and wake interaction may result in unsteady forces of significant size on both the impeller blades and the diffuser vanes. If the radial gap between the impeller blades and the diffuser vanes is small both interaction mechanisms will occur simultaneously, and will influence each other.

Most of the work on blade row interaction with the aim of measuring unsteady blade pressures has been carried out on axial turbomachinery. Among others, Dring et al. (1982) investigated blade row interaction in an axial turbine and found both potential flow and wake interaction for closely spaced blade rows (15% based on chord). Significant pressure fluctuations of up to 72% of the exit dynamic pressure were measured near the leading edge of the rotor. Gallus (1979) and Gallus et al. (1980) reported measurements on axial compressors. The blade rows were spaced relatively far apart (60% based on chord), such that the potential flow interaction between the rotor and the stator was weak; i.e., the pressure fluctuations on the compressor stator were found to be considerably larger than those on the compressor rotor. In radial turbomachinery, impeller blade pressure measurements were reported by Iino and Kasai (1985). The radial gap between the impeller blades and the diffuser vanes was small, so that significant pressure fluctuations on the impeller blades were observed. Furthermore, it was found that blade and vane angle have an important influence on the blade pressure fluctuations. Flow field investigations in centrifugal compressors have been reported among others by Inoue and Cumptsy (1984) and Stein and Rautenberg (1988). Diffuser vane pressure measurements using the impeller of the High Pressure Turbopump of the Space Shuttle Main Engine were made by Arndt et al. (1988). Experiments were made for radial gaps of 1.5% and 4.5% (based on the impeller discharge radius) between the impeller blades and the diffuser vanes. The pressure fluctuations were found to be of the same order of magnitude as the total pressure rise across the pump.

To investigate the complete rotor–stator interaction mechanism, unsteady pressure measurements have to be made on both the impeller blades and the diffuser vanes. In this paper, the results of such measurements using a two–dimensional centrifugal test impeller and different vaned radial diffusers will be presented. To the authors knowledge, this is the first pub-

* Presently with MTU (Motoren– und Turbinen Union München GmbH), Postfach 500640, 8000 München 50, Federal Republic of Germany.

Presented at the Gas Turbine and Aeroengine Congress and Exposition—June 4-8, 1989—Toronto, Ontario, Canada
This paper has been accepted for publication in the Transactions of the ASME
Discussion of it will be accepted at ASME Headquarters until September 30, 1989

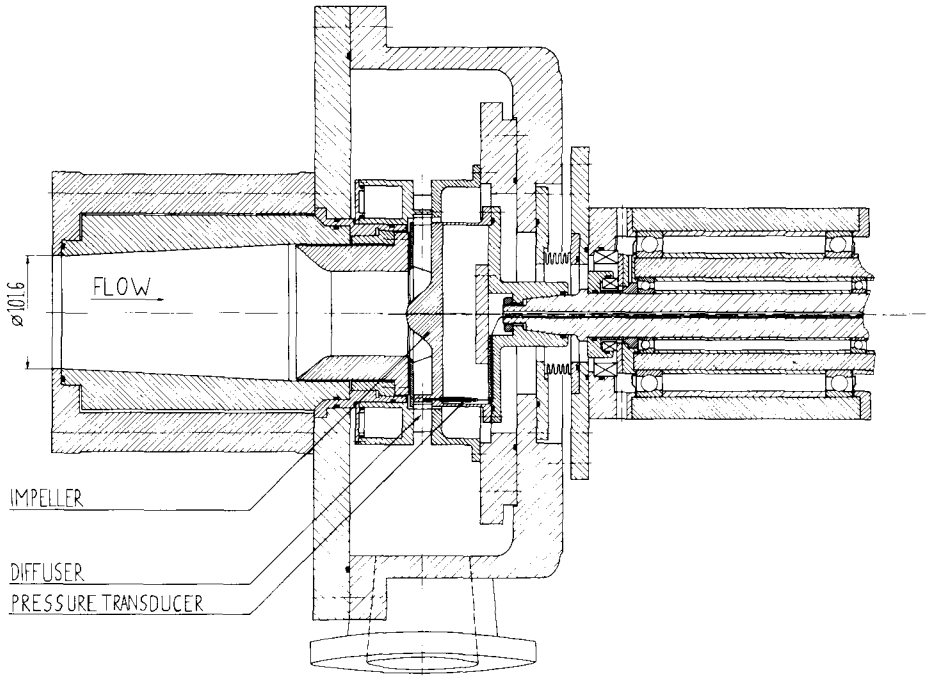

Fig. 1 Assembly drawing of the eccentric drive system and the test section with Impeller Z2 installed.

NOMENCLATURE

a_i, b_i	coefficient of the ith cos and the ith sin term in a Fourier series, normalized by $(1/2)\rho u_2^2$
A_2	impeller discharge area
b_2	impeller discharge width
b_3	diffuser inlet width
c	vane chord
c_b	blade pressure coefficient, $c_b = p_b/(1/2)\rho u_2^2$
c_i	magnitude of ith Fourier coefficient, $c_i = \sqrt{a_i^2 + b_i^2}$
c_L	lift coefficient, $c_L = L/(1/2)\rho u_2^2 c$
$\overline{c}_p$	steady vane pressure coefficient, $\overline{c}_p = (\overline{p}_v - \overline{p}_{up})/(1/2)\rho u_2^2$
$\tilde{c}_p$	unsteady vane pressure coefficient, $\tilde{c}_p = \tilde{p}_v/(1/2)\rho u_2^2$
$\tilde{c}_{p,av}$	ensemble averaged unsteady vane pressure coefficient, $\tilde{c}_{p,av} = \tilde{p}_{v,av}/(1/2)\rho u_2^2$
$c_{p,av}$	ensemble averaged vane pressure coefficient, $c_{p,av} = \overline{c}_p + \tilde{c}_{p,av}$
d_2, d_3	impeller discharge diameter, diffuser inlet diameter
$\mathbf{F}$	force vector on diffuser vane
f	frequency
f_b	impeller blade passage frequency, $f_b = z_b(rpm/60)$
f_s	shaft frequency, $f_s = (rpm/60)$
f_v	impeller blade passage frequency, $f_v = z_v(rpm/60)$
L	lift (component of the force vector on the vane normal to the chord joining the vane leading edge and the vane trailing edge)
p, p_t	pressure, total pressure
Q	flow rate
R	radius
R_2	impeller discharge radius
R_3	diffuser inlet radius
R_{mean}	mean line radius of the circular arc vanes
rpm	revolutions per minute
t_v	vane thickness
u_2	impeller tip speed, $u_2 = 2\pi R_2(rpm/60)$
x, y	diffuser vane coordinates
z_b, z_v	number of impeller blades, number of diffuser vanes
α^*	impeller blade trailing edge angle (= impeller blade angle)
β^*	diffuser vane leading edge mean line angle (= diffuser vane angle)
ξ	parametric diffuser vane coordinate
ρ	density
φ_i	phase of ith Fourier coefficient, $\varphi_i = \tan^{-1}(a_i/b_i)$
ϕ	flow coefficient, $\phi = Q/u_2 A_2$
ψ	total head coefficient, $\psi = (p_{down} - p_{up})/\rho u_2^2$
ω	radian frequency, $\omega = 2\pi f$

Subscripts

av	ensemble averaged
b	impeller blade
$down$	downstream
max	maximum
s	shaft
up	upstream
v	diffuser vane

Superscripts

$\overline{\ }$	steady
$\tilde{\ }$	unsteady

Abbreviations

FP	pressure side of impeller blade
FS	suction side of impeller blade
LE	diffuser vane leading edge
PCB	PCB Piezoelectronics, INC. Depew, NY 14043
PS	diffuser vane pressure side
SS	diffuser vane suction side
TE	diffuser vane trailing edge

lication reporting both unsteady impeller blade and unsteady diffuser vane pressure measurements in a diffuser pump. All measurements were obtained for noncavitating flow.

Data will be presented on steady and unsteady diffuser vane pressure measurements along mid vane height. Superimposing the steady and ensemble averaged unsteady vane pressure, the ensemble averaged vane pressure was obtained (it was assumed that the steady pressure value measured with mercury manometers was identical to the time mean pressure about which the piezoelectric pressure transducers, used for the unsteady measurements, measure the unsteady pressure). Steady and unsteady computations of the force on the vane were made from those pressure measurements. A second two-dimensional impeller, referred to as Impeller Z2, with the same blade number and the same blade geometry as Impeller Z1, was used for the impeller blade pressure measurements. For those measurements, different diffuser vane configurations were used to investigate the influence of the vane number and the vane leading edge mean line angle (also referred to as vane angle) on the impeller blade pressure fluctuations.

During the tests, the impellers could only be positioned at locations on an orbit concentric to the diffuser center (orbit radius=1.27 mm), so that the radial gap between the impeller blade trailing edge and the leading edge of any instrumented diffuser vane could be varied between 5% and 8% of the impeller discharge radius. Similarly, for the impeller blade pressure measurements, the radial gap between the instrumented impeller blade and the diffuser vanes varied between 5% and 8% of the impeller discharge radius during one impeller revolution. Are the blade and vane pressure fluctuations measured for the "local" radial gaps between the impeller blades and diffuser vanes representative for diffuser pumps in which the radial gap between the impeller blades and diffuser vanes is uniform? During one shaft revolution the impeller flow is subjected to disturbances at two different frequencies (low frequency disturbances such as rotating stall etc. are excluded from this discussion since the present investigation did not focus on such phenomena); namely a disturbance due to the presence of the diffuser vanes occurring at vane passage frequency, f_v, and a disturbance due to the varying radial gap between the impeller blades and diffuser vanes during one shaft revolution occurring at shaft frequency, f_s. For the centrifugal pump stages investigated, the vane passage frequency was an order of magnitude larger than the shaft frequency ($6 \leq (f_v/f_s) \leq 12$). Hence, it is inferred that the flow about an impeller blade passing a diffuser vane at a certain radial gap can be considered "quasiperiodic." That is to say the pressure fluctuations experienced by a particular impeller blade and a particular diffuser vane are representative of the pressure fluctuations the impeller blades and the diffuser vanes experience in diffuser pumps with a uniform radial gap. The proximity of neighboring diffuser vanes (for the instrumented impeller blade) and neighboring impeller blades (for the instrumented diffuser vane) with a slightly different radial gap is considered to be a small perturbation with only a small effect on the blade and vane pressure fluctuations measured on the particular instrumented impeller blade and diffuser vane.

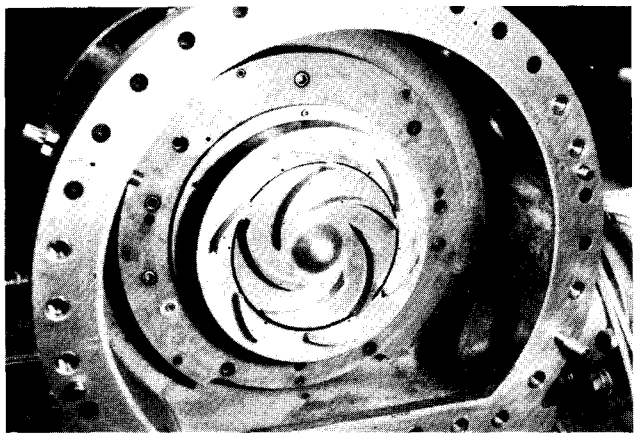

Fig. 2 Photograph of Impeller Z2 and Diffuser G installed in the test section (the front shroud of the impeller was removed to show the impeller blade shapes).

TEST FACILITY AND INSTRUMENTATION

The experiments were conducted in a recirculating water test loop. The facility has been in detail described by Arndt (1988). A simplified view of the test section with the two-dimensional test impeller for impeller blade pressure measurements, Impeller Z2, installed is shown in figure 1.

Table 1 Impellers.

Impeller	z_b	α^*	d_2 (mm)	b_2 (mm)
Imp. Z1	5	25°	161.92	15.75
Imp. Z2	5	25°	161.92	15.75

The two two-dimensional impellers have identical blade number and identical blade shape (five logarithmic spiraled blades with a blade angle of 25 degrees). Impeller Z1 existed from previous work when the current investigation was started, and was used for most of the diffuser vane pressure measurements, but difficult to modify for impeller blade pressure measurements. Subsequently, Impeller Z2 was designed and built to permit impeller blade pressure measurements by mounting pressure transducers to the impeller. A photograph of Impeller Z2 installed in the test facility is shown in figure 2 (the front shroud of the impeller was removed to show the impeller blade shapes). Impeller blade pressure measurements were made at three pressure taps on the impeller blades, one on the blade pressure side ($R/R_2 = 0.987$), one at the impeller blade trailing edge ($R/R_2 = 1.0$), and one on the impeller blade suction side ($R/R_2 = 0.937$). The signals from the pressure transducers were transmitted by cables from the pressure transducers to a slip ring assembly and from there to the pressure transducer power supply.

Diffuser vane pressure measurements were made using a straight wall constant width diffuser with nine vanes, referred to as Diffuser S. No volute, however, is provided. Thus, the flow is discharged from the diffuser into a large housing. The shape of a vane, with the pressure taps at mid vane height, is shown in figure 3. It is identical to the one used in an early version of the diffuser of the High Pressure Oxygen Turbopump (HPOTP) of the Space Shuttle Main Engine (SSME); however, the number of diffuser vanes was reduced from seventeen to nine. Unsteady vane pressure measurements using this diffuser and one half of the double suction pump impeller of the HPOTP of the SSME have been reported by Arndt et al. (1988).

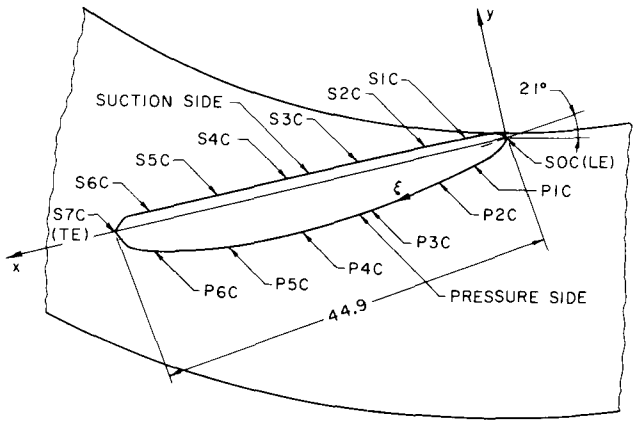

Fig. 3 Diffuser vane with pressure taps at mid vane height.

A second diffuser, of identical side wall geometry and diffuser channel width as Diffuser S, but permitting variable diffuser vane configurations was used to investigate the effects of the number of diffuser vanes and of the vane leading edge mean angle (also referred to as the vane angle), β^*, on the impeller blade pressure measurements. This diffuser employed circular arc vanes with the geometry listed in table 2.

Table 2 Geometry of the Circular Arc Vanes.

R_{mean}	88.91 mm
c	56.90 mm
t_v	4.19 mm

Four different diffusers were used for the unsteady impeller blade pressure measurements (diffuser vane pressure measurements could only be made with Diffuser S); the details are listed in table 3. In figure 2, a photograph showing Impeller Z2, with the front shroud removed to show the impeller blade shapes, and Diffuser G is presented.

Table 3 Diffusers.

Diffuser	Vane Type	z_v	β^*	d_3 (mm)	b_3 (mm)
Diff. F	cir. arc	12	20°	172.72	14.99
Diff. G	cir. arc	6	20°	172.72	14.99
Diff. H	cir. arc	6	10°	172.72	14.99
Diff. S	see fig.3	9	21°	172.72	14.99

Steady pressure measurements were obtained by using conventional mercury manometers. The wall pressure about 350 mm upstream of the impeller inlet, $\bar{p}up$, was used as reference pressure. The experimental error on the steady pressure measurements, i.e., on $(\bar{p} - \bar{p}up)$, was estimated to be $\pm 0.5\%$ of $(\bar{p} - \bar{p}up)$.

Piezoelectric pressure transducers with built–in amplifiers from PCB Inc. were used for the unsteady measurements. This particular transducer (Model 105B02) was selected because of its small size (diaphragm diameter: 2.54 mm), high resonant frequency (250 kHz), and high resolution ($\sim 70N/m^2$). Because of the relatively short discharge time constant of the transducer of 1 sec., static calibration means could not be used. Instead, the dynamic calibration provided by the manufacturer was used. The linearity of the calibration was within 2%. The resonant frequency of the impeller blade and the diffuser vane pressure taps, the geometry of which is shown in figure 4, was estimated to be approximately 8000 Hz. The spectrum of unsteady pressure measurements (figure 5) shows that the estimate of the resonant frequency was reasonable. It can be seen that the blade passage frequency and its higher harmonics are "far" removed from the resonant frequency of the pressure tap, so that amplification and phase shift were negligible.

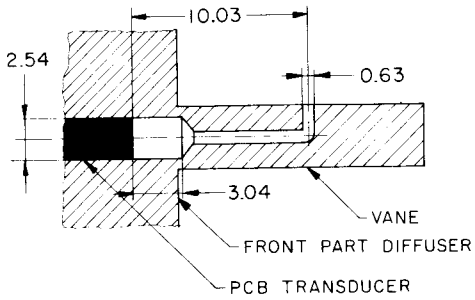

Fig. 4 Geometry of the diffuser vane and impeller blade pressure taps.

The data were sampled and discretized in a 16 channel data acquisition system. An encoder on the main shaft was used to trigger the data acquisition system and to provide a clock for the data acquisition system. 1024 data points were taken during one shaft revolution. Since the signal contained some noise, the unsteady data were ensemble averaged over one impeller revolution. The experimental error was found to be less than $\pm 5\%$ for the magnitude and less than $\pm 2\%$ (360 degrees corresponding to one impeller blade passage) for the phase of the ensemble averaged unsteady pressure measurements.

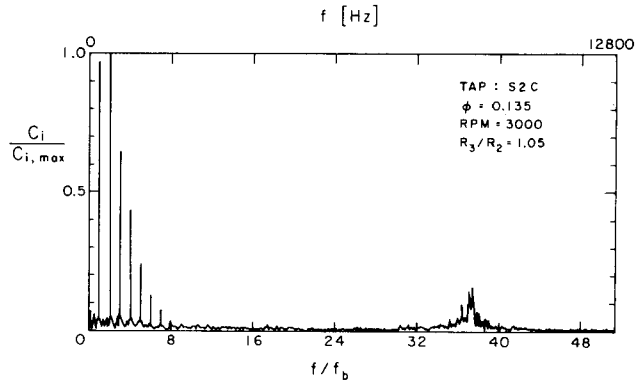

Fig. 5 Spectrum of unsteady diffuser vane pressure measurements for Impeller Z1 and Diffuser S at pressure tap S2C ($\phi = 0.135, R_3/R_2 = 1.05$, rpm $= 3000$).

OVERALL PERFORMANCE

Performance curves for Impeller Z2 and the different vaned diffusers are shown in figure 6. The largest flow coefficients were obtained using Diffuser S (the modified SSME diffuser) and Diffuser G ($z_v = 6, \beta^* = 20°$). For those diffusers, the head rise for large flow coefficients, $\phi \geq 0.9$, was larger than for Diffuser F ($z_v = 12, \beta^* = 20°$) and for Diffuser H ($z_v = 6, \beta^* = 10°$). For low flow coefficients, $\phi \leq 0.07$, Diffuser F had the largest head rise. Diffuser H had the smallest head rise of all diffusers in the range of flow coefficients investigated.

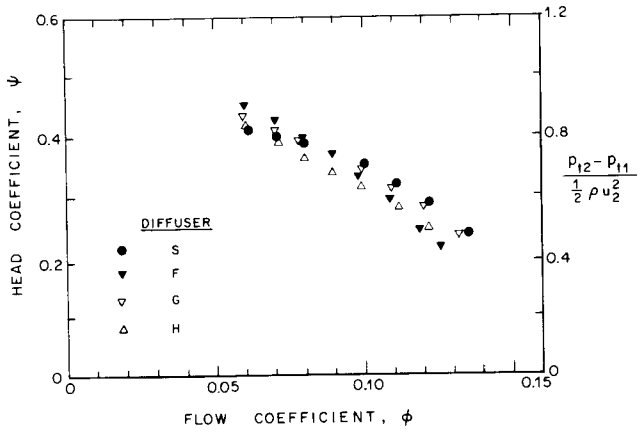

Fig. 6 Performance curves for Diffusers F,G,H and S.

DIFFUSER VANE PRESSURE MEASUREMENTS FOR DIFFUSER S

Steady Vane Pressure Measurements and Steady Vane Lift Computations. The steady vane pressure measurements are presented as a steady pressure coefficient, normalized by the dynamic pressure based on impeller tip speed, $(1/2)\rho u_2^2$,

$$\bar{c}_p = \frac{\bar{p}_v - \bar{p}_{up}}{(1/2)\rho u_2^2}.$$

Steady diffuser vane pressure measurements were made for three flow coefficients, $\phi = 0.135, 0.10$ and 0.06, two radial gaps between diffuser vanes and impeller blades (5% and 8% of the impeller discharge radius) and a rotational speed of 1200 rpm. The steady vane pressure distribution for the medium flow coefficient, $\phi = 0.10$, is shown in figure 7. The pressure distribution on the vane changes only slightly with increasing radial gap. Furthermore, the diffusion on the vane suction side can clearly be seen.

From the steady vane pressure measurements at mid vane height, the steady force on the vane at mid vane height was computed. The steady pressure distribution around the vane was obtained by fitting a third order periodic spline through the measured data. A periodic spline fit was chosen to get continuity for the pressure and the first two pressure derivatives at the vane leading and the vane trailing edge. Hence, the steady force was computed from

$$\overline{\mathbf{F}} = -\oint (\overline{p}_v - \overline{p}_{up})(\xi)\mathbf{n}d\xi.$$

The lift on the vane was defined as the component of the force on the vane normal to the chord joining the vane leading and the vane trailing edge. The lift on the vane was defined as positive if the force component normal to the vane chord was in the positive y direction (figure 3). The lift is presented as a lift coefficient, normalized by the dynamic pressure based on impeller tip speed, $(1/2)\rho u_2^2$, and the vane chord, c,

$$\overline{c}_L = \frac{L}{(1/2)\rho u_2^2 c}.$$

The steady lift on the diffuser vane versus flow coefficient vanes is shown in figure 8. It can be seen that the steady lift increases significantly with decreasing flow coefficient. With the exception of the lowest flow coefficient, $\phi = 0.06$, the steady lift and moment decrease slightly with increasing radial gap.

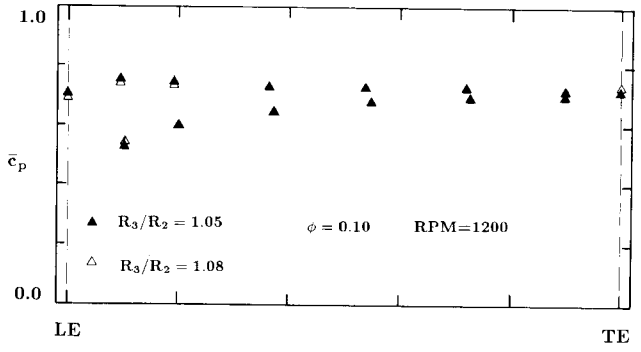

Fig. 7 Steady pressure measurements at mid vane height for Impeller Z1 and Diffuser S ($\phi = 0.10, R_3/R_2 = 1.05$ and 1.08, rpm = 1200).

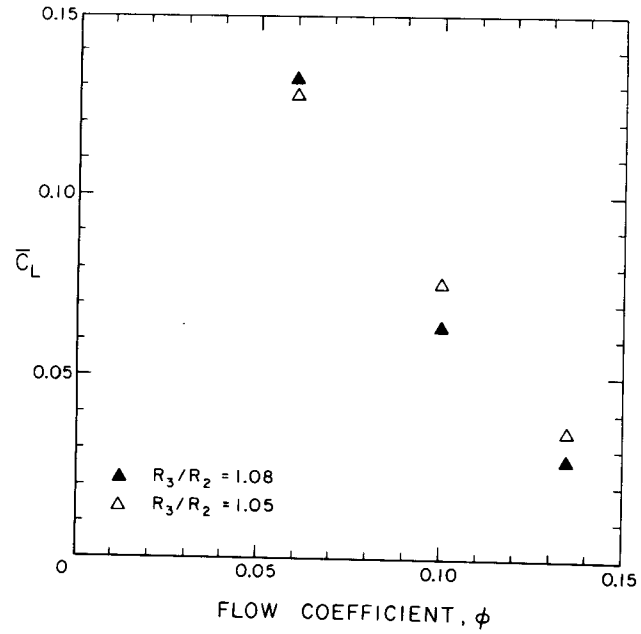

Fig. 8 Steady lift coefficient versus flow coefficient for Impeller Z1 and Diffuser S ($R_3/R_2 = 1.05$ and 1.08, rpm = 1200).

Ensemble Averaged Unsteady Vane Pressure Measurements and Spectra of Unsteady Vane Pressure Measurements. The unsteady vane pressure measurements were ensemble averaged, and will be presented as an ensemble averaged vane pressure coefficient, normalized by the dynamic pressure based on impeller tip speed,

$$\tilde{c}_{p,av}(i) = \frac{1}{N}\sum_{j=1}^{N} \frac{\tilde{p}_v(i,j)}{(1/2)\rho u_2^2},$$

where N is the number of averaging periods, i the ith data point taken in any of the N averaging periods, and j the jth of the N averaging periods. During one averaging period, corresponding to one main shaft revolution (or five impeller blade passages), 1024 data points were taken. A total of 512 averaging periods was used for the ensemble averages. Furthermore, spectra of the unsteady data were obtained. In figure 9, a sample of the ensemble averaged vane pressure fluctuations is presented. The measurements were made at pressure tap S2C, for the medium flow coefficient, $\phi = 0.10$, and $R_3/R_2 = 1.05$ (the pressure tap S2C was selected since the largest vane pressure fluctuations occurred at that measurement location). The ensemble averaged vane pressure fluctuations are shown in the upper half of the figure. The position of the impeller blades is referenced to the diffuser vane leading edge. The magnitude of the Fourier coefficients relative to the magnitude of the largest Fourier coefficient ($c_i/c_{i,max}$) is shown versus frequency (upper horizontal scale) and frequency normalized by impeller blade passage frequency (f/f_b) (lower horizontal scale) in the lower half of the figure.

It is evident that the pressure fluctuations are periodic with the impeller blade passage frequency, and of the same order of magnitude as the total pressure rise across the pump. The largest pressure at this particular measurement location (S2C) occurs right before the pressure side of the impeller blade trailing edge reaches the diffuser vane leading edge. As the blade trailing edge passes the vane leading edge, the pressure decreases sharply and attains its minimum as the suction side of the blade trailing edge reaches the vane leading edge. Then, the pressure rises sharply as the impeller blade moves away from the vane leading edge. Hence, most of the pressure fluctuations occur during a rather short time, corresponding to about one third of the impeller blade passage period. The spectrum of the unsteady pressure measurements at tap S2C is dominated by the impeller blade passage frequency and its higher harmonics. In fact, the second harmonic is slightly larger than the first.

Magnitude of Ensemble Averaged Diffuser Vane Pressure Fluctuations. In the following figures, data on the magnitude of the ensemble averaged unsteady vane pressure measurements at vane mid height are presented. The magnitude of the pressure fluctuations is defined as the difference between the maximum and minimum pressure value in the averaging period, which corresponds to one impeller revolution. The largest fluctuations, independently of flow coefficient or radial gap, occur at the vane leading edge and on the front half of the vane suction side. Those fluctuations are of the same order of magnitude as the total pressure rise across the pump. The fluctuations are larger on the vane suction than on the vane pressure side. On the vane pressure side, they decrease monotonically from the leading edge to the trailing edge, whereas on the vane suction side they have a relative minimum at pressure tap S1C, and they decrease from pressure tap S2C monotonically to the vane trailing edge. For the two flow coefficients investigated, the largest fluctuations occur either at the vane leading edge or at pressure tap S2C.

Figure 10 shows the dependence of the fluctuations on the radial gap between impeller blades and diffuser vanes, $R_3/R_2 = 1.05$ and 1.08, for $\phi = 0.10$ and 3000 rpm. The large pressure fluctuations on the front half of the suction side, at the leading edge and at the pressure tap on the pressure side closest to the leading edge decrease significantly with increasing radial gap. However, at the pressure taps on the rear half of the vane suction side and at the other pressure taps on the pressure side, the pressure fluctuations remain virtually unchanged.

Figure 11 compares the fluctuations for the two flow coefficients, ϕ = 0.135 and 0.10, at 3000 rpm and R_3/R_2 = 1.05. At the leading edge and at all pressure taps on the suction side, the fluctuations are larger for ϕ = 0.135 than for ϕ = 0.10. With the exception of pressure tap P1C, where the fluctuations are larger for ϕ = 0.10 than for ϕ = 0.135, the magnitude of the pressure fluctuations on the vane pressure side is nearly identical for the two flow coefficients.

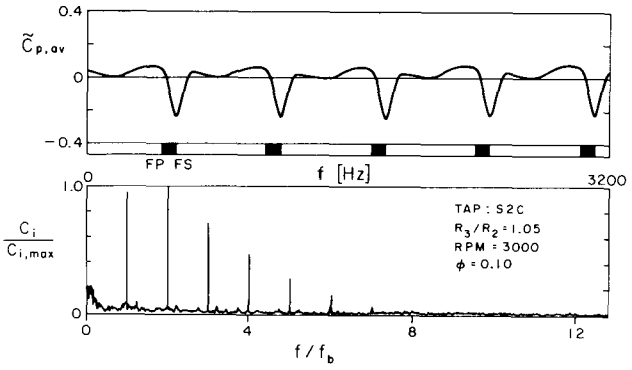

Fig. 9 Ensemble averaged unsteady vane pressure measurements and spectrum of unsteady vane pressure at pressure tap S2C for Impeller Z1 and Diffuser S (ϕ = 0.10, R_3/R_2 = 1.05, rpm = 3000).

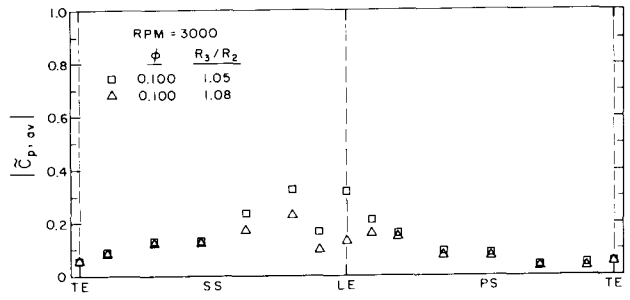

Fig. 10 Magnitude of ensemble averaged vane pressure fluctuations at mid vane height for Impeller Z1 and Diffuser S (ϕ = 0.10, R_3/R_2 = 1.05 and 1.08, rpm = 3000).

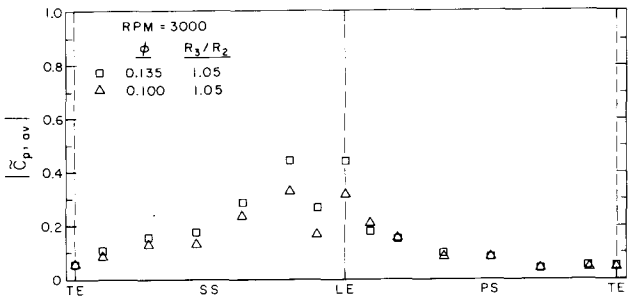

Fig. 11 Magnitude of ensemble averaged vane pressure fluctuations at mid vane height for Impeller Z1 and Diffuser S (ϕ = 0.135 and 0.10, R_3/R_2 = 1.05, rpm = 3000).

For one pressure tap, S2C, unsteady vane pressure measurements were made over a range of flow coefficients, ranging from maximum flow coefficient, ϕ_{max} = 0.135, to ϕ = 0.06. The shaft speed during those tests was 1500 rpm (comparing the normalized pressure measurements for ϕ = 0.135 and 0.10 made at 1500 and 3000 rpm, virtually no shaft speed dependence was found). In figure 12, the magnitude of the fluctuations as functions of flow coefficient and radial gap, relative to the magnitude of the fluctuation for maximum flow, ϕ = 0.135, at a radial gap of 5%, are presented. It can be seen that the fluctuations are largest for the maximum flow coefficient and decrease with decreasing flow coefficient. Increasing the radial gap between impeller blades and diffuser vanes resulted in an about 50% decrease of the fluctuations. Comparing the normalized total pressure rise across the pump (figure 6) to the normalized impeller blade pressure fluctuations, it can be seen that the magnitude of the vane pressure fluctuations for the maximum flow coefficient, ϕ = 0.135, is about 95% of the total pressure rise across the pump.

Steady and unsteady diffuser vane pressure measurements using one half of the double-suction pump of the High Pressure Oxygen Turbopump of the Space Shuttle Main Engine were reported by Arndt et al. (1988). The vane pressure fluctuations, for comparable radial gaps between impeller blades and diffuser vanes were found to be of similar magnitude.

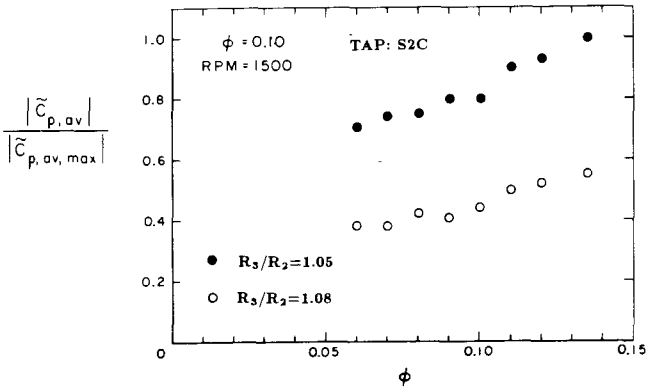

Fig. 12 Magnitude of ensemble averaged vane pressure fluctuations at pressure tap S2C for Impeller Z1 and Diffuser S (ϕ = 0.06 − 0.135, R_3/R_2 = 1.05 and 1.08, rpm = 1500).

Magnitude and Phase of Fourier Coefficients of Ensemble Averaged Vane Pressure Fluctuations. The magnitude and the phase of the Fourier coefficients corresponding to impeller blade passage frequency, f_b, twice impeller blade passage frequency, $2f_b$, and three times the impeller blade passage frequency, $3f_b$, will be presented for the medium flow coefficient, ϕ = 0.10, and a radial gap of 5%. A curve is drawn through the data points in figures 14 and 15 (magnitude and phase of the blade passage harmonics). The drawn curve has no significance other than to connect the data points as an aid in viewing the data.

The magnitudes of the Fourier coefficients are presented in figure 14. Note that the vertical scale, for the magnitude of the coefficients, is not a linear but a logarithmic one. The magnitude of the first harmonic, i.e., the impeller blade passage harmonic, is approximately equal at most pressure taps on the front half of the vane suction and the vane pressure side (taps P1C, P2C, S0C, S2C and S3C). The magnitudes of the second and third blade passage harmonics, however, are significantly larger on the front half of the vane suction than on the vane pressure side. In fact, the magnitude of the second harmonic at the pressure taps on the front half of the vane suction side is as large or larger than the magnitude of the first harmonic. On the rear half of the vane suction side, the magnitude of the first harmonic is, however, significantly larger than the second harmonic. In contrast, on the rear half of the vane pressure side, the magnitude of the second harmonic is larger than the magnitude of the first harmonic.

Hence, the higher impeller blade passage harmonics do contribute significantly to the diffuser vane pressure fluctuations and cannot be neglected in an analysis.

The phase angle of the blade passage harmonics is shown in figure 15. The reference configuration, i.e., the geometric configuration at which the data taking process was started, is schematically shown in figure 13. It can be seen that there is a significant difference in phase, of $\approx$ 70 degrees, between the first impeller blade passage harmonic on the front half of the vane suction side and the front half of the vane pressure side.

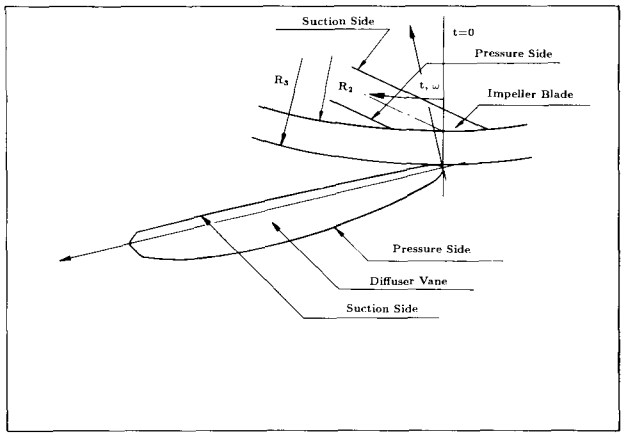

Fig. 13 Geometric reference configuration for phase computation.

Ensemble Averaged Lift Computations. From the vane pressure measurements described earlier, the force on the vane at mid vane height was computed. Since those measurements were obtained on different vanes, they had to be phase shifted to one reference vane for the force computations. Superimposing the steady and ensemble averaged unsteady pressure measurements, the ensemble averaged vane pressure distribution was obtained. From the ensemble averaged pressure distribution, the ensemble averaged force was computed. The ensemble averaged pressure distribution on the vane was obtained by fitting a third order periodic spline through the measured pressure values. A periodic spline fit was chosen to get continuity for the pressure and the first two pressure derivatives at the leading and trailing edge. The ensemble averaged force was computed from

$$\mathbf{F_{av}} = -\oint (\overline{p}_v + \tilde{p}_{v,av} - \overline{p}_{up})(\xi)\mathbf{n}d\xi.$$

The lift on the vane was defined as the component of the force on the vane normal to the chord joining the vane leading and trailing edge. The lift on the vane was defined as positive if the force component normal to the vane chord was in positive y direction (figure 3). The ensemble averaged lift is presented as an ensemble averaged lift coefficient, normalized by the dynamic pressure based on impeller tip speed, $(1/2)\rho u_2^2$, and the vane chord, c,

$$c_{L,av} = \frac{L_{av}}{(1/2)\rho u_2^2 c}.$$

In figures 16 and 17 data on the ensemble averaged lift and on the ratio of ensemble averaged to steady lift are presented. The position of the impeller blade is referenced to the diffuser vane leading edge. The averaging period for ensemble averaging was one shaft revolution, corresponding to five impeller blade passages; the data for the first half of shaft revolution are presented.

In figure 16, the ensemble averaged lift for the two flow coefficients investigated, $\phi = 0.135$ and $\phi = 0.10$, is shown for a radial gap of 5%. It can be seen that the lift fluctuations are larger for the maximum flow coefficient than for the medium flow coefficient. Minimum lift is attained as the pressure side of the impeller blade trailing edge reaches the vane leading edge. As the blade trailing edge passes the vane leading edge, the lift increases from its minimum to its maximum value which is attained as the suction side of impeller blade trailing edge reaches the vane leading edge. As the impeller blade moves away from the diffuser vane trailing edge, the lift does first decrease to approximately its mean value. Then the lift stays relatively constant for about a third of the blade passage period before dropping to its minimum value.

This behavior, i.e., the relatively constant lift on the diffuser vane for a significant part of the impeller blade passage period, is in contrast to the results on diffuser lift fluctuations using one half of the double suction impeller of the High Pressure Oxygen Turbopump of the Space Shuttle Main Engine and Diffuser S (Arndt et al. 1988). For the impeller of the SSME, the lift on a diffuser vane of the same diffuser decreased strongly monotonically from its maximum to its minimum value. The impeller of the SSME has more blades, eight in contrast to five of Impeller Z1. Hence, due to the fewer num-

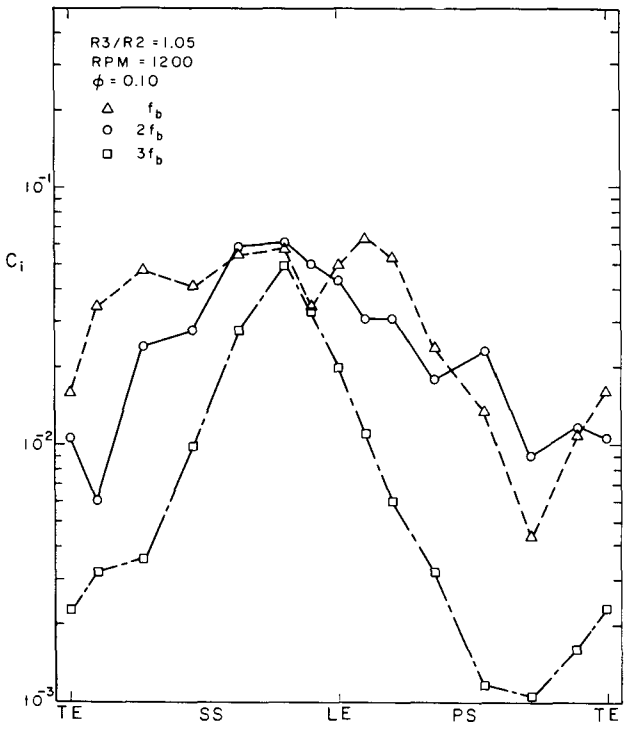

Fig. 14 Magnitude of the Fourier coefficients of impeller blade passage harmonics for Impeller Z1 and Diffuser S ($\phi = 0.10, \mathbf{R_3/R_2} = 1.05$, rpm $= 1200$).

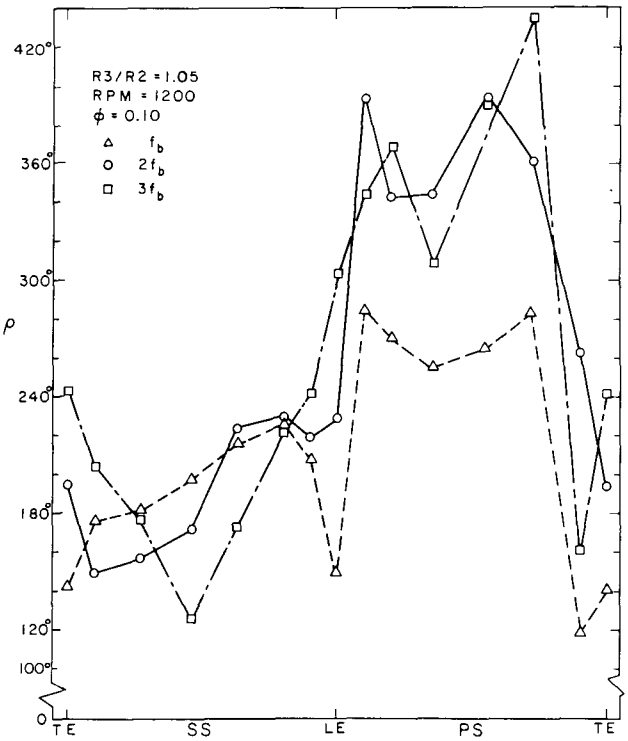

Fig. 15 Phase of the Fourier coefficients of impeller blade passage harmonics for Impeller Z1 and Diffuser S ($\phi = 0.10, \mathbf{R_3/R_2} = 1.05$, rpm $= 1200$).

ber of impeller blades there is an interval of time in a blade passage period during which the influence of the impeller blade–diffuser vane interaction on the unsteady lift is small; i.e, the ensemble averaged pressure distribution about the vane was observed to be nearly identical to the steady pressure distribution about the vane ($c_{p,av} \approx \bar{c}_p$). The magnitude of the lift fluctuations, however, was found to be approximately equal for the two impellers for comparable flow coefficients and radial gaps between impeller blades and diffuser vanes.

The ratio of the ensemble averaged lift to the steady lift for the medium flow coefficient, $\phi = 0.10$, and radial gaps of 5% and 8% is shown in figure 6.17. For both radial gaps, the ratio is about 2, decreasing slightly with increasing radial gap.

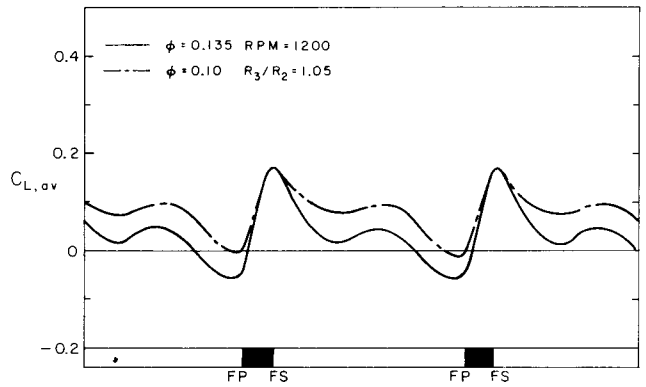

Fig. 16 Ensemble averaged lift on the diffuser vane at vane mid height for Impeller Z1 and Diffuser S ($\phi = 0.10$ and $0.135, \mathbf{R_3/R_2} = 1.05$, rpm $= 1200$).

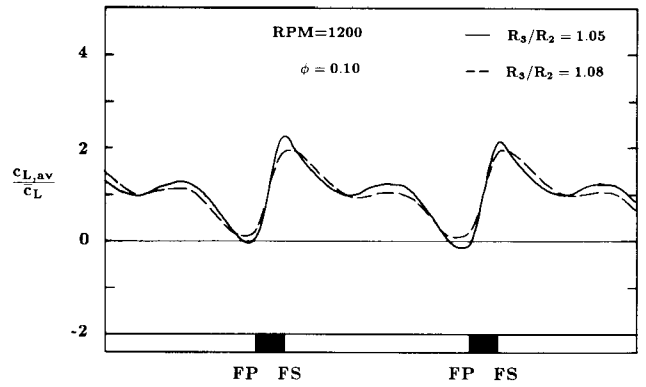

Fig. 17 Ratio of ensemble averaged lift to steady lift on the diffuser vane at vane mid height for Impeller Z1 and Diffuser S ($\phi = 0.10, \mathbf{R_3/R_2} = 1.05$ and 1.08, rpm $= 1200$).

UNSTEADY IMPELLER BLADE PRESSURE MEASUREMENTS USING DIFFUSER S

Unsteady impeller blade pressure measurements were made at three pressure taps on the impeller blades, one on the pressure side ($R/R_2 = 0.987$), one on the suction side ($R/R_2 = 0.937$), and one on the trailing edge ($R/R_2 = 1.00$). Herein, the measurements made for Diffuser S and the two-dimensional impeller are presented. Data were taken for eight flow coefficients, ranging from $\phi = 0.135$ to $\phi = 0.06$ at 1500 rpm. Since the impeller was positioned eccentrically to the diffuser center, the radial gap between impeller blade trailing edge and diffuser vane leading edge varied during one impeller revolution from 5% to 8% of the impeller discharge radius.

Ensemble Averaged Unsteady Blade Pressure Measurements and Spectra of Unsteady Blade Pressure Measurements. Similar to the unsteady vane pressure measurements, the unsteady blade pressure measurements were ensemble averaged, and will be presented as an ensemble averaged blade pressure coefficient, normalized by the dynamic pressure based on impeller tip speed. Furthermore, spectra of the unsteady measurements were obtained.

In figure 18, the ensemble averaged unsteady blade pressure measurements and the corresponding spectrum of the unsteady blade pressure measurements at the blade trailing edge pressure tap are presented for a medium flow coefficient, $\phi = 0.10$. In the upper part, the ensemble averaged blade pressure fluctuations are shown. The pairs of broken lines indicate the passage of the pressure side and the suction side of the impeller blade trailing edge past the diffuser vane leading edge. The one pair of solid lines indicates the passage of the pressure side and the suction side of the impeller blade trailing edge past the diffuser vane leading edge at the smallest radial distance between the instrumented impeller blade and the diffuser vanes. That smallest radial gap between the impeller blade trailing edge and the diffuser vane leading edge is 5% of the impeller discharge radius. In the lower part of the figure, the magnitude of the Fourier coefficients relative to the largest Fourier coefficient ($c_i/c_{i,max}$) is shown versus frequency (upper horizontal scale) and frequency normalized by impeller vane passage frequency (f/f_v) (lower horizontal scale).

It can be seen that the magnitude of the fluctuations varies significantly during one impeller revolution. This is due to the varying distance between the impeller blade trailing edge and the diffuser vane leading edges as the impeller completes one revolution. The trailing edge pressure fluctuations are largest during the vane passage following the smallest gap between the specific instrumented impeller blade and the diffuser vanes. The minimum pressure at the trailing edge pressure tap within each diffuser vane passage is attained after the impeller blade trailing edge has passed the diffuser vane leading edge. The trailing edge pressure then rises sharply to its maximum value which is attained before the impeller blade trailing edge reaches the next vane leading edge.

In the corresponding spectrum of the unsteady blade pressure measurements, four different discrete frequency components can be found. First, vane passage frequency and its higher harmonics, $(f/f_v) = 1, 2...$, are the dominant frequencies. This is similar to the diffuser vane pressure measurements presented previously. Secondly, a component at shaft frequency, f_s, can be seen. This component results from the varying radial gap between the impeller blades and the diffuser vanes as the impeller completes one shaft revolution. Thirdly, frequencies at $mf_v \pm nf_s (n, m = 1, 2)$ can have significant magnitude. These frequencies are the result of frequency modulation between the vane passage frequency, f_v, and the shaft frequency, f_s,

$$\sin(2\pi f_v t)\sin(2\pi f_s t) = 0.5(\cos((f_v - f_s)2\pi t) - \cos((f_v + f_s)2\pi t)$$

and hence result from the uneven radial gap between impeller blades and diffuser vanes. Fourthly, a strong 60 Hz signal and some very small higher harmonics can be seen. The 60 Hz is significantly larger than for the diffuser vane pressure measurements. The larger 60 Hz signal may be due to the

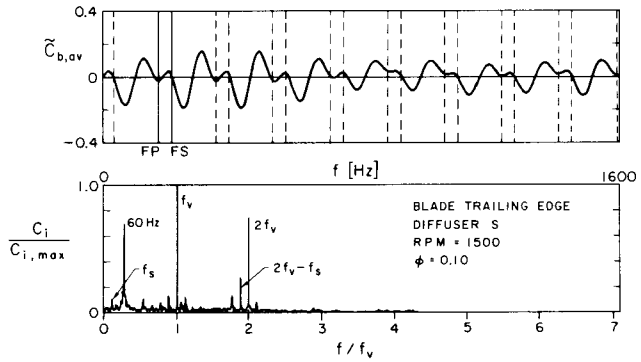

Fig. 18 Ensemble averaged unsteady blade pressure measurements and spectrum of unsteady blade pressure measurements at the blade trailing edge pressure tap for Impeller Z2 and Diffuser S ($\phi = 0.10$, rpm $= 1500$).

60 Hz motor speed control. That is, because of the 60 Hz output of the motor control the drive shaft may induce both flow oscillations around the impeller blades and impeller vibrations at 60 Hz, which may be picked up by the transducer. Since the 60 Hz signal was very sharp and sufficiently far removed from the shaft frequency and vane passage frequency, it was not expected to influence the measurements. During the ensemble averaging process, the 60 Hz signal was processed out.

Magnitude of Ensemble Averaged Blade Pressure Fluctuations. For the smallest radial gap, $R_3/R_2 = 1.05$, that is the closest position between the impeller blade and a diffuser vane as the impeller completes one revolution, the magnitudes of the ensemble averaged blade pressure fluctuations are presented in figure 19. The measurements were made for a total of eight flow coefficients, ranging from maximum flow, $\phi = 0.135$, to $\phi = 0.06$.

It can be seen that the magnitudes of the pressure fluctuations range from the same order of magnitude as the total pressure rise across the pump at the trailing edge pressure tap, to an order of magnitude smaller than the total pressure rise across the pump at the suction side pressure tap.

The largest fluctuations occur at the trailing edge. They increase significantly with decreasing flow coefficient, from $|\tilde{c}_{b,av}| = 0.17$ for $\phi = 0.135$ (maximum flow) to $|\tilde{c}_{b,av}| = 0.46$ for $\phi = 0.07$. Comparing the normalized total pressure rise across the pump as a function of flow coefficient (figure 6) to the normalized impeller blade pressure fluctuations as a function of flow coefficient, it can be observed that the magnitude of the pressure fluctuations can be as large as about 60% of the total pressure rise across the pump. Thus, the impeller blade pressure fluctuations can be of the same order of magnitude as the diffuser vane pressure fluctuations.

In contrast to the trailing edge pressure fluctuations, the pressure fluctuations at the pressure and suction side pressure taps are not significantly dependent upon flow coefficient. Maxima are attained for $\phi = 0.11$ at the pressure side pressure tap, for $\phi = 0.10$ at the suction side pressure tap, and for $\phi = 0.06$ at the suction and pressure side pressure tap. Minima are attained for maximum flow, $\phi = 0.135$, at both the pressure and suction side pressure tap, and for $\phi = 0.09$ at the pressure side pressure tap, and for $\phi = 0.08$ at the suction side pressure tap. The magnitude of the fluctuations at the pressure and suction side pressure tap, however, was found to be quiet different. At the pressure side pressure tap, the fluctuations were about two to three times larger than at the suction side pressure tap. For maximum flow, the fluctuations at the pressure side pressure tap were even slightly larger than those at the trailing edge pressure tap. Not increasing significantly with decreasing flow coefficient, however, the fluctuations at the pressure side pressure tap for low flow coefficients were only about half as large as those at the trailing edge pressure tap.

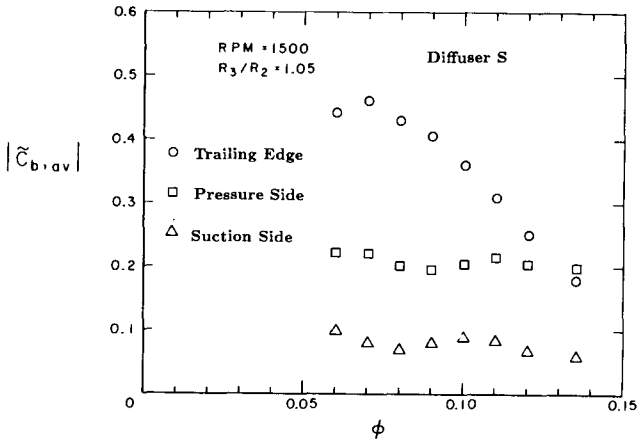

Fig. 19 Magnitude of ensemble averaged pressure fluctuations at the three impeller blade pressure taps for Impeller Z2 and Diffuser S ($\phi = 0.06 - 0.135, R_3/R_2 = 1.05$, rpm = 1500)

UNSTEADY IMPELLER BLADE PRESSURE MEASUREMENTS USING DIFFERENT DIFFUSERS.

Unsteady impeller blade pressure measurements were also made for a second diffuser, of identical sidewall geometry as Diffuser S, but permitting variable diffuser vane configurations. Three different vane configurations employing circular arc vanes were tested (see also table 3). Diffuser F employed twelve vanes with a vane angle, β^*, of twenty degrees, Diffuser G six vanes with a vane angle of twenty degrees, and Diffuser H six vanes with a vane angle of ten degrees. Hence, the different diffuser vane configurations permitted an investigation of the influence of the diffuser vane number and of the diffuser vane angle on the impeller blade pressure fluctuations.

Magnitude of Ensemble Averaged Blade Pressure Fluctuations. The influence of the different diffuser vane configurations on the unsteady impeller blade pressure measurements is presented in figure 20 for the trailing edge pressure tap, in figure 21 for the pressure side pressure tap, and in figure 22 for the suction side pressure tap. The largest pressure fluctuations occurred independently of the diffuser vane configuration at the impeller blade trailing edge. The number of the diffuser vanes and the diffuser vane angle, however, were observed to have a significant influence on the pressure fluctuation at all three impeller blade pressure taps. The increase in vane number from six to twelve at a fixed vane angle of 20 degrees resulted in a decrease of the blade pressure fluctuations at all blade pressure taps and for all flow coefficients. The reduction varied, depending upon flow coefficient and pressure tap, between 15% and 70%. At the trailing edge and at the pressure side pressure tap, the fluctuations decreased more strongly for the lower flow coefficients, whereas at the suction side pressure tap the fluctuations decreased more strongly at the pressure side pressure tap. Decreasing the vane angle from 20 degrees to 10 degrees for a constant number of diffuser vanes ($z_v = 6$) resulted for the pressure taps on the blade pressure and on the blade suction side in an increase of the pressure fluctuations for the large flow coefficients of up to 75%, whereas for low flow coefficients the fluctuations decreased by up to 30%. For the trailing edge pressure tap, the magnitude of the pressure fluctuations remained unchanged for large flow coefficients and decreased for low flow coefficients.

Discussion of the Impeller Blade Pressure Measurements. The impeller blade pressure fluctuations are assumed to be primarily the result of the potential interaction between the diffuser vanes and the impeller blades (Dring 1982 and Gallus 1980). This was qualitatively confirmed by the unsteady impeller blade pressure measurements presented herein.

From the steady vane pressure measurements for Diffuser S, a significant increase in the lift on the diffuser vanes (and hence of the circulation about a diffuser vane) was observed when the flow coefficient was reduced (figure 8). Hence, the circulation about a single diffuser vane, sensed by the rotating impeller blades as a periodic fluctuation, was found to increase with decreasing flow coefficient. This may cause the increase of the pressure fluctuations at the blade trailing edge with decreasing flow coefficient observed for the unsteady impeller blade pressure measurements using Impeller Z2 and Diffuser S (figure 19).

Increasing the number of diffuser vanes in a vaned diffuser results in a decrease of the loading of a single diffuser vane. Therefore, also the circulation about a single diffuser vane, sensed by the rotating impeller blades as a periodic fluctuation, decreases. Comparing the results of the unsteady impeller blade pressure measurements for Impeller Z2 and Diffuser F ($z_v = 12, \beta^* = 20°$) and Impeller Z2 and Diffuser G ($z_v = 6, \beta^* = 20°$), it can be seen that the impeller blade pressure fluctuations, at all three pressure taps and for the entire range of flow coefficients investigated, were smaller for the twelve–vaned than for the six–vaned diffuser (figures 20–22). This is very likely the result of the reduced circulation about a single diffuser vane, and may therefore confirm that the impeller blade pressure fluctuations are primarily the result of the potential flow interaction between impeller blades and diffuser vanes.

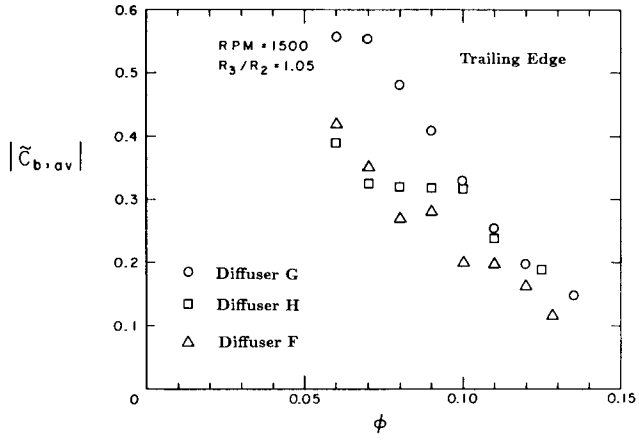

Fig. 20 Magnitude of ensemble averaged pressure fluctuations at the pressure tap at the impeller blade trailing edge for Impeller Z2 and Diffusers F, G and H ($\phi = 0.06 - 0.135, R_3/R_2 = 1.05$, rpm = 1500).

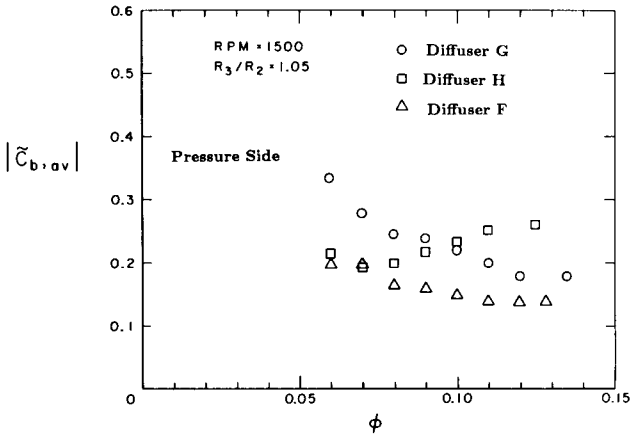

Fig. 21 Magnitude of ensemble averaged pressure fluctuations at the pressure tap at the impeller blade pressure side for Impeller Z2 and Diffusers F, G and H ($\phi = 0.06 - 0.135, R_3/R_2 = 1.5$, rpm = 1500).

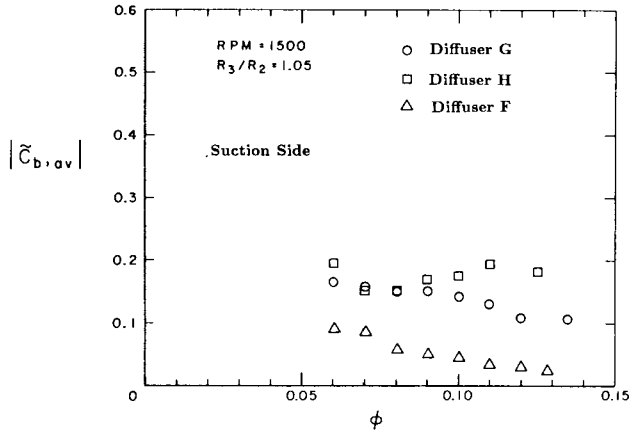

Fig. 22 Magnitude of ensemble averaged pressure fluctuations at the pressure tap at the impeller blade suction side for Impeller Z2 and Diffusers F, G and H ($\phi = 0.06 - 0.135, R_3/R_2 = 1.05$, rpm = 1500).

SUMMARY AND CONCLUSION

An experimental investigation of unsteady flow in a centrifugal pump with different vaned diffusers was carried out focusing on impeller blade–diffuser vane interaction. Steady and unsteady diffuser vane pressure measurements were made for a two–dimensional test impeller and a vaned diffuser for radial gaps of 5% and 8% of the impeller discharge radius.

It was found that:

- The pressure fluctuations were larger on the suction side than on the pressure side.
- The largest vane pressure fluctuations occurred on the vane suction side close to the leading edge. For a large flow coefficient, $\phi = 0.135$, and a radial gap of 5%, the magnitude of those fluctuations reached $\approx 95\%$ of the total pressure rise across the pump for that particular flow coefficient.
- Increasing the radial gap between impeller blades and diffuser vanes from 5% to 8% resulted in a significant decrease of the large pressure fluctuations on the front half on the vane suction side.
- The fluctuating lift on the diffuser vane was about twice as large as the steady lift.

Unsteady impeller blade pressure measurements were made for a second two–dimensional test impeller with blade number and blade geometry identical to the two–dimensional impeller used for the diffuser vane pressure measurements, but permitting pressure transducers to be mounted to the impeller. Those measurements were made for the vaned diffuser used for the diffuser vane pressure measurements and a second diffuser of identical side wall geometry but permitting variable diffuser vane geometry to investigate the influence of the vane number and the influence of the vane angle on the impeller blade pressure fluctuations.

- The largest blade pressure fluctuations occurred at the impeller blade trailing edge, independently of the diffuser vane configuration.
- Those fluctuations increased significantly with decreasing flow coefficient, in contrast to the large pressure fluctuations at the diffuser vane suction side which decreased with decreasing flow coefficient. For a low flow coefficient, $\phi = 0.06$, and a radial gap of 5%, the magnitude of those fluctuations reached $\approx 60\%$ of the total pressure rise across the pump for that particular flow coefficient.
- Increasing the vane number from six to twelve resulted in a significant decrease of the blade pressure fluctuations at all blade pressure taps (with the exception of low flow coefficients, the total pressure rise across the pump, however, was reduced as a result of the increased vane number).
- Decreasing the vane angle from twenty degrees to ten degrees (for six diffuser vanes) resulted in a decrease of the large pressure fluctuations at the blade trailing edge, and in an increase of the pressure fluctuations at the suction side pressure tap (the total pressure rise across the pump, however, was reduced as a result of the decreased vane angle for all flow coefficients investigated).

In summary, it was found that pressure fluctuations, of the same order of magnitude as the total pressure rise across the pump, can occur on the impeller blades and the diffuser vanes if the radial gap between the impeller blades and the diffuser vanes is small, i.e., of the order of a small percentage of the impeller discharge radius. The large pressure fluctuations at the impeller blade trailing edge may be responsible for the cavitation damage occurring at the trailing edges of the impeller blades. Furthermore, it was shown that the fluctuating lift on the diffuser vanes can be larger than the steady lift. For high speed, high performance pumps with closely spaced blade rows, this result should be considered in the structural design of the vane.

ACKNOWLEDGEMENTS

The authors are indebted to the NASA George Marshall Space Flight Center for the continued sponsorship of this research under contract NAS8–33108.

REFERENCES

Arndt, N., "Experimental Investigation of Rotor–Stator Interaction in Diffuser Pumps," Ph.D. Thesis, Division of Engineering and Applied Science, California Institute of Technology, 1988.

Arndt, N., Acosta, A.J., Brennen, C.E., and Caughey, T.K., "Rotor–Stator Interaction in a Diffuser Pump," 33rd ASME International Gas Turbine and Aeroengine Congress (88–GT–55), June 5–9, 1988, Amsterdam, and to appear in the ASME *Journal of Turbomachinery*.

Dring, R.P., Joslyn, H.D., Hardin, L.W., and Wagner, J.H., "Turbine Rotor–Stator Interaction," ASME *Journal of Engineering for Power*, Oct. 1982, Vol. 104, pp. 729–742.

Gallus, H.E., "High Speed Blade–Wake Interactions," *von Kármán Institute for Fluid Mechanics Lecture Series 1979–9*, Jan. 29–Feb. 2, 1979, Vol. 2.

Gallus, H.E., Lambertz, J., and Wallmann, T., "Blade Row Interaction in an Axial Flow Subsonic Compressor Stage," ASME *Journal of Engineering for Power*, Jan. 1980, Vol. 102, pp. 169–177.

Iino, T., and Kasai, K., "An Analysis of Unsteady Flow Induced by Interaction Between a Centrifugal Impeller and a Vaned Diffuser," (in Japanese), *Transactions of the Japan Society of Mechanical Engineers*, 1985, Vol. 51, No. 471, pp. 154–159.

Inoue, M., and Cumptsy, N.A., "Experimental Study of Centrifugal Impeller Discharge Flow in Vaneless and Vaned Diffusers," ASME *Journal of Engineering for Gas Turbines & Power*, April 1984, Vol. 106, pp. 455–467.

Lefcort, M.D., "An Investigation into Unsteady Blade Forces in Turbomachines," ASME *Journal of Engineering for Power*, Oct. 1965, Vol. 20, pp. 345–354.

Stein, W., and Rautenberg, M., "Analysis of Measurements in Vaned Diffusers of Centrifugal Compressors," ASME *Journal of Turbomachinery*, Jan. 1988, Vol. 110, No. 1, pp. 115–121.